Journal of
Mechanical
Science and
Technology

Journal of Mechanical Science and Technology 21 (2007) 970~975

Dynamic Stair Walking of Biped Humanoid Robots

Seungchul Lim*

Department of Mechanical Engineering, Myongi University, San 38-2, Namdong, Yongin, 449-728, Korea

(Manuscript Received November 16, 2006; Revised January 8, 2007)

Abstract

Biped humanoid robots are expected to move around human-centered setting that includes stairs as a major terrain. Reportedly, however, only few of them can walk up and down stairways as of now. Making it worse, even the successful ones carry out such motions either barely in terms of speed or fast enough but in an undisclosed technical manner. In this context, a dynamic gait pattern is proposed anew suitable for stair walks along with a transient pattern and verified by means of a multi-body dynamics analysis software.

Keywords: Stair walking; Biped; Inverted pendulum model; ZMP; Hyperbolic and polynomial patterns

1. Introduction

For sufficient versatility, it is essential for biped humanoid robots to move around human-centered setting that includes stairs as a major terrain. Reportedly, however, only few of them can walk up and down stairways as of now. Making it worse, even the successful ones carry out such motions either barely in terms of speed (Bae, 2001) or fast enough but in an undisclosed technical manner (Hirai *et al.*, 1998).

The key to stair walking seems how to solve the unusual dynamic stability problem arising from coupling effects between vertical and horizontal motions, which does not appear in the case of planar locomotions maintaining constant robot height. To circumvent such a stability issue, most sluggish robots tend to take quasi-static gait patterns at the expense of large actuator torque.

In this context, a dynamic gait pattern is here proposed anew suitable for stair walks. To this end, the popular inverted pendulum model (Lim *et al.*, 2005 ; Loffler *et al.*, 2003 ; Vukobratovic *et al.*, 1990) is adopted to approximate dynamics of a 12-DOF biped robot of typical design. Next, equilibrium conditions about a point usually termed ZMP (Zero Moment Point) are applied to derive the ZMP constraint equation. Upon solving the equation with relevant inputs, hyperbolic trajectories for 3-D body motions are analytically obtained securing dynamic stability. In addition, a transient pattern of polynomial type is introduced applicable to smooth assembly of various motions with the steady one.

Subsequently, foot locations are planned in consideration of terrain shape and ZMP positions. Remarkably at times, the ZMP may exist off actual staircases so that it could be quite different from the ones prescribed as if 2-D planar cases. Once trajectories of the body and feet are prepared, joint motions can be computed based on inverse kinematics in the literature (Lim *et al.*, 2005). Finally distributed mass and ground contact effects on such joint-space motions are evaluated by means of a multi-body dynamics analysis software (Mechanical Dynamics, 2001). Simulation results verify the effectiveness of proposed gait patterns.

*Corresponding author. Tel.: +82 31 330 6428, Fax.: +82 31 321 4959
E-mail address: slim@mju.ac.kr

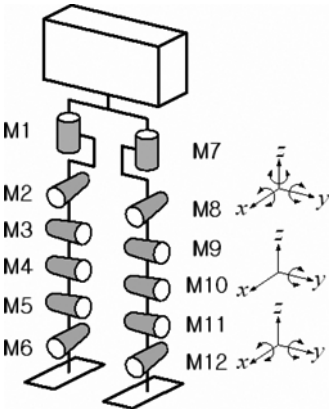

Fig. 1. Skeleton diagram of the robot.

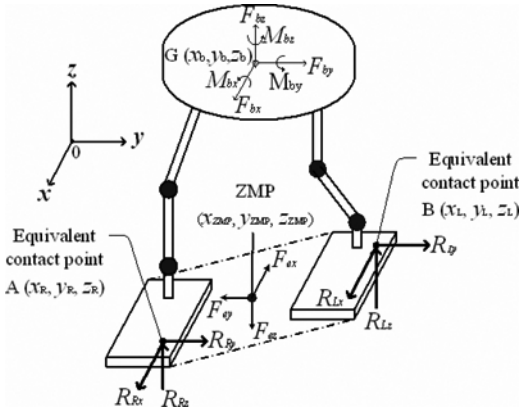

Fig. 2. Biped robot walking on a 3-D terrain.

2. Robot structure and walking patterns

The biped robot under present investigation has a torso and duplicate legs of 6 DOFs as in Fig. 1. In effect, first three of the rotational axes orthogonally intersect at the pelvis joint, next one at the knee, and the last two at the ankle by such elements as timing belts. Moreover, they are arranged in sequence of yaw (M1/M7), roll (M2/M8), pitch (M3/M9), pitch (M4/M10), pitch (M5/M11), and roll (M6/M12) downward from the top.

Walking on regular stairways, robots will undergo periodic motions. Hence they need a stable steady gait pattern. However, robots in practice change up locomotion styles from one to another. For this reason, a stable transient pattern is also meaningful. Both are to be detailed henceforth.

2.1 Steady pattern

To secure stability during dynamic gaits, robots have to satisfy the ZMP constraint equation (Vukobratovic *et al.*, 1990). However, its form may vary depending on applications.

Refer to Fig. 2 for a 3-D case. By applying equilibrium conditions about ZMP point in conjunction with the inverted pendulum model approach, one can set up the following equations along horizontal directions of the inertial Cartesian coordinate frame. In so doing, note that all the reaction forces from the ground can be ignored.

$$M_{bx} - F_{by}(z_b - z_{ZMP}) - F_{bz}(y_{ZMP} - y_b) = 0,$$
$$M_{by} + F_{bx}(z_b - z_{ZMP}) + F_{bz}(x_{ZMP} - x_b) = 0 \quad \text{(1a,b)}$$

where $F_{bx} = -m\ddot{x}_b$, $F_{by} = -m\ddot{y}_b$, $F_{bz} = -m\ddot{z}_b - mg$, with m the total mass lumped at point G, and also $M_{bx} = M_{by} = 0$ assuming no tipping angular acceleration of the body. As a result, the ZMP equation in search turns out as below.

$$\ddot{x}_b - c^2 x_b = -c^2 x_{ZMP},$$
$$\ddot{y}_b - c^2 y_b = -c^2 y_{ZMP} \quad \text{(2a,b)}$$

which the coefficient $c^2 = (\ddot{z}_b + g)/(z_b - z_{ZMP})$ in coupled the vertical and horizontal motions unlike the familiar 2-D cases.

Although the robot height inevitably changes with time on stairs, it's advisable to render c constant somehow. If so, motions along horizontal directions can be treated as if straight planar walking (Lim *et al.*, 2005). Hence, one might as well focus only on vertical motion from this point on. Meanwhile, above definition of c leads to an extra relationship regarding the vertical motion described by $z_{bM}(= z_b - g/c^2)$:

$$\ddot{z}_{bM} - c^2 z_{bM} = -c^2 z_{ZMP} \quad \text{(2c)}$$

In summary, Eq. (2) constitutes a full 3-D set of ZMP equations that are mutually independent but identical in forms. Hence, as with Eqs. (2a) and (2b), Eq. (2c) can be solved for vertical motion of the upper body taking the ZMP position as an input, i.e.,

$$z_{bM}(t) = (z_{bM0} - z_{ZMP})\cosh ct + \frac{\dot{z}_{bM0}}{c}\sinh ct + z_{ZMP} \quad (3)$$

Obviously, z_{bM0} and $\dot{z}_{bM0}$ respectively denote the initial position and velocity.

As sketched in Fig. 3, distinct motional strategies are established depending on how the robot is suppor-

ted. During DSP (double support phase), the robot maintains not only a uniform velocity in each direction but also a constant height with each supportive foot on neighboring stair. On the other hand, during SSP (single support phase) the robot proceeds with a variable speed and height until it recovers the normal height relative to the next stair, which is sized H along z direction.

Accordingly, dynamic effect is to be involved along vertical direction during SSP alone. To deal with it, each SSP is divided into 3 subintervals of positive, zero, and negative acceleration successively numbered as I, II, and III. Ensuring smooth motions up to velocities across all intervals provides Eq. (4).

$$c(z_{bM0} - z_{ZMPS1})\sinh ct_1 = v_z, \tag{4a}$$

$$c(z_{bMt2} - z_{ZMPS2})\cosh ct_3 + \frac{v_z}{c}\sinh ct_3 + z_{ZMPS2} = z_{bM0} + H, \tag{4b}$$

$$c(z_{bMt2} - z_{ZMPS2})\sinh ct_3 + v_z\cosh ct_3 = 0, \tag{4c}$$

where the total of 7 unknowns are c, v_z ($=\dot{z}_{bM}$ at the end of I), z_{ZMPS1} and z_{ZMPS2} (ZMP positions during I and III respectively), t_1, t_2 & t_3 (time duration of each subinterval), and another notation to identify is z_{bMt2} ($=z_{bM}$ at the end of II). Taking into account that the three time durations are normally determined by desired horizontal motions (Lim *et al.*, 2005), and c can be set to $\sqrt{g/z_{b0}}$ as in planar walking, the remaining 3 unknowns can be found as solutions of a linear algebraic equation without difficulty.

A feature to emphasize is that the such-obtained vertical ZMP positions could exist off the stair terrain. To clarify this point, revisit Fig. 2. Regardless of supportive phase, the reaction forces acting on point A and B statically balance those at ZMP by definition. In other words,

$$F_{ex} = R_{Lx} + R_{Rx},\quad F_{ey} = R_{Ly} + R_{Ry},$$
$$F_{ez} = R_{Lz} + R_{Rz}, \tag{5a,b,c}$$

$$-R_{Lz}(y_{ZMP} - y_L) + R_{Rz}(y_R - y_{ZMP}) + R_{Ly}(z_{ZMP} - z_L) - R_{Ry}(z_R - z_{ZMP}) = 0, \tag{5d}$$

$$R_{Lz}(x_{ZMP} - x_L) - R_{Rz}(x_R - x_{ZMP}) - R_{Lx}(z_{ZMP} - z_L) + R_{Rx}(z_R - z_{ZMP}) = 0. \tag{5e}$$

In turn, with z_{ZMP} available as a constant Eq. (5) can give

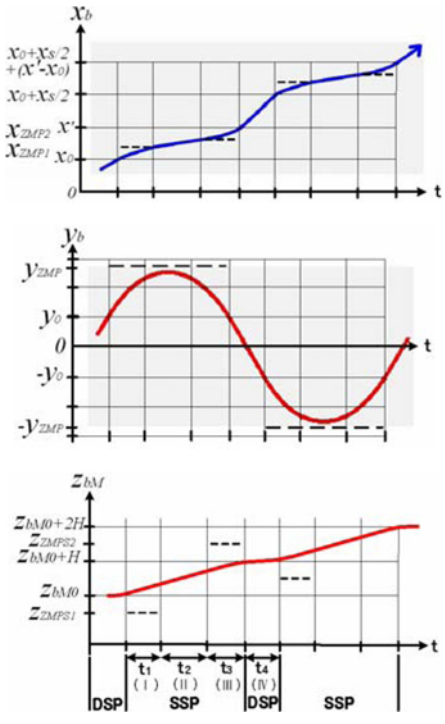

Fig. 3. Hyperbolic walking pattern.

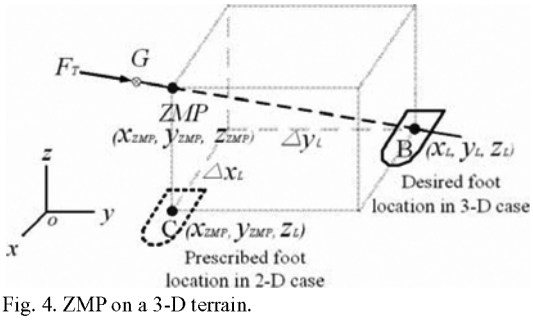

Fig. 4. ZMP on a 3-D terrain.

Table 1. Specifications of the robot.

Part	Size [mm]	Mass [kg]
Body	196(W)×150(H)×60(T)	17.81
Right Leg	325(L)	2.150
Left Leg	325(L)	2.150
Right Foot	50(W)×110(L)×3(T)	0.1546
Left Foot	50(W)×110(L)×3(T)	0.1546
Total	-	22.42

$$x_{ZMP} = \frac{R_{Lz}x_L + R_{Rz}x_R}{F_{ez}} + \frac{R_{Lx}(z_{ZMP} - z_L) + R_{Rx}(z_{ZMP} - z_R)}{F_{ez}}, \tag{6a}$$

$$y_{ZMP} = \frac{R_{Lz} y_L + R_{Rz} y_R}{F_{ez}} + \frac{R_{Ly}(z_{ZMP} - z_L) + R_{Ry}(z_{ZMP} - z_R)}{F_{ez}}. \quad (6b)$$

Indeed, x_{ZMP} and y_{ZMP} in Eq. (6) together correspond to ZMP position to be prescribed through planning process of horizontal motion, while first terms on the right hand sides do the desired equivalent contact point (or center of reaction forces) on terrain surface at the same level (Lim et al., 2005). Now, for brevity suppose that the robot is in SSP by the left foot. Then $R_{Rx} = R_{Ry} = R_{Rz} = 0$, and $F_{ez} = R_{Lz}$ as well so that Eq. (6) can be reduced as below.

$$x_{ZMP} = x_L + \Delta x_L, \quad y_{ZMP} = y_L + \Delta y_L, \quad (7a,b)$$

where Δx_L and Δy_L quantify the amount by which the prescribed ZMP position deviates from the desired point to cover by the left foot. Such are further illustrated in Fig. 4; in case z_{ZMP} lies above the left foot, the ZMP will serve to indicate the direction of the resultant applied force, F_T, along with the robot's center of gravity marked as point G. Consequently, it's reasonable to place the left foot on the terrain at point B rather than C.

As long as the horizontal reaction forces such as R_{Lx} and R_{Ly} can be made small enough by careful walking patterns, however, those offset terms may be bounded by the stability margin. From simulations, it was observed that the larger stairs are, the more unstable the robot goes especially sideways. To resolve such a problem, it is also advisable slowing down walking speed.

2.2 Transient pattern

Robots in skillful operation need to change up locomotion styles from one to another. To reflect this, the selected robot is assumed to initially stand still right ahead of stairs with both feet in parallel, and after a few steps come to rest on stairway again in DSP. Then the robot should be equipped with any stable transient pattern to assemble such postures with the foregoing steady pattern.

Although a hyperbolic pattern was already suggested for similar purposes (Lim *et al.*, 2005), a simpler yet still effective method is to be introduced. Basically this approach uses a cubic polynomial to smoothly connect body motions across the transient period concerned. For instance, one may employ the following function of time along x-direction:

$$x_b(\tau) = a_3\tau^3 + a_2\tau^2 + a_1\tau + a_0, \quad (8)$$

where the involved four coefficients depend upon initial and final conditions of position and speed. It is noteworthy that the time duration, t^*, decisively influences stability of transient motion. So, it's always required to see whether ZMPs calculated by Eqs. (8) and (4) are inside the stable region a priori. To make the most of broader stable region, application of the transient pattern is recommendable for traverses between DSPs as in the present case.

3. Dynamics simulations

The selected biped robot is 478mm tall and weighs 22.4kg, about 80% of which belongs to the torso. For more details, refer to Table 1. As in the work (Lim *et al.*, 2005), the normal reaction force from ground contact is modeled as the sum of nonlinear spring and viscous damping forces. Besides, thrust force is regarded to take place in form of Coulomb friction whose friction coefficient equals either 0.8 or 0.7 depending on slip velocity.

As an example, relevant gait parameters are inputted: z_b =300mm, x_0 =0, x_s = 275mm, $x_{ZMP1} = x_s/20$, $x_{ZMP2} = x_s/10$, y_{ZMP} =68mm, v_{xD} =110mm/s, c =5.7155/s, t^* =0.5s, and H =20mm. In return, the relevant equations by Lim *et al.* (2005) compute $t_1 = t_3$ =0.1568s, t_2 =0.1786s, t_4 =0.8750s so that steady walking period becomes 1.3672s. For the simulation time of 5.59s including four continuous steps, body position and velocity evolve as in Figs. 5 and 6.

Meanwhile, ZMP positions throughout entire time turn out well inside the stable region as evidenced in Figs. 7 and 8. In relation, foot trajectories along x & z-directions were smoothly planned as in Figs. 9 and 10, and as can be known in Fig. 7 the foot trajectory along y-direction stays constant.

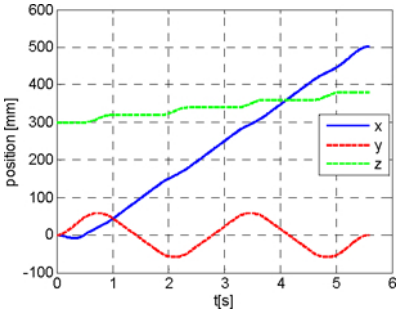

Fig. 5. Body positions.

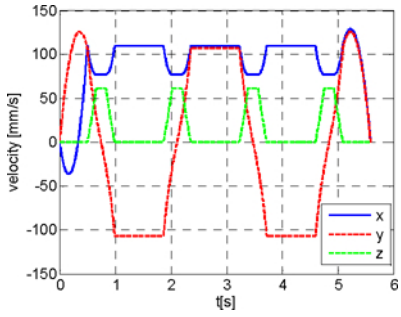

Fig. 6. Body velocities.

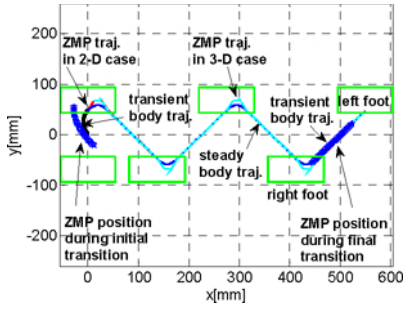

Fig. 7. Position trajectory (XY plot).

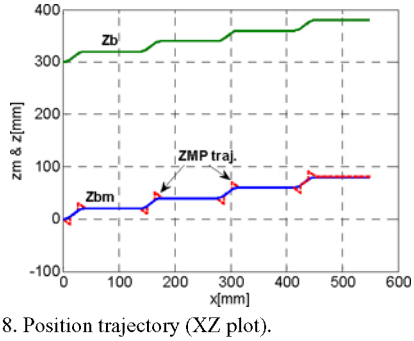

Fig. 8. Position trajectory (XZ plot).

As for the ZMP offsets during steady period, Fig. 11 reconfirms those smaller than the stability margin (or foot size) and relatively large toward side direction. Next two figures exhibit dynamic simulation results obtained by use of ADAMS. Figure 12 shows the 3-D torso motions with no body shaking. Comparisons between Figs. 5 and 12 imply that stair walking is well performed as planned with only a momentary difference at the beginning, which is ascribable to abrupt knee bending to prepare for locomotion. Displayed in Fig. 13 are the snapshots of animated walking motion captured every second. Since the average walking speed is about 1s/step during steady periods, almost each frame visualizes alternate postures.

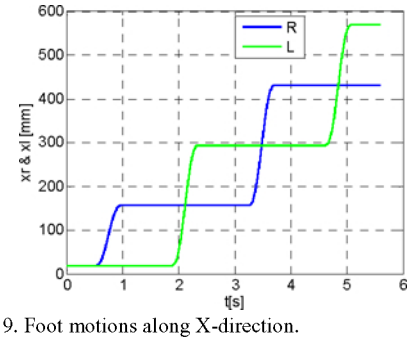

Fig. 9. Foot motions along X-direction.

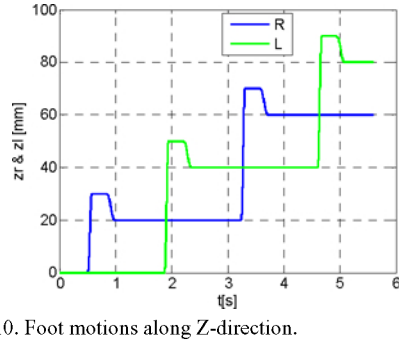

Fig. 10. Foot motions along Z-direction.

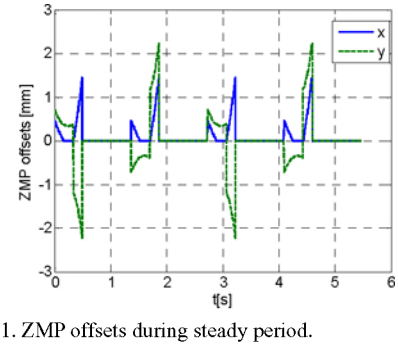

Fig. 11. ZMP offsets during steady period.

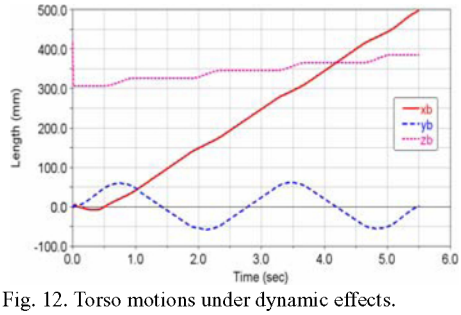

Fig. 12. Torso motions under dynamic effects.

4. Conclusions

A hyperbolic dynamic walking pattern is proposed anew applicable to biped robots for stair

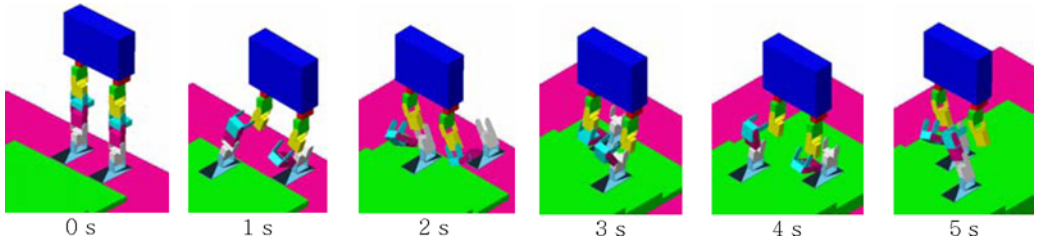

Fig. 13. Snapshots of the stair walking.

walking. In addition, a polynomial transient pattern is supplement to smoothly assemble the initial and final stationary postures with the steady locomotion. Remarkably, it is discussed how much ZMP could exist off the actual terrain in the case of 3-D walking, and what measure needs to be taken in response. As an example, a typical biped robot of height 478mm has been successfully simulated under dynamic effects. It walks up stairs at an average speed near 1s per step sized 20mm tall and 138mm deep.

Acknowledgements

This work was supported by Korea Science and Engineering Foundation Grant (KOSEF-R-01-2003-000-10014-0). The author is grateful for the support.

References

Bae, J. H., 2001, "A Study on the Stair Walking of Lower Power Biped Robot," *KIEE/IEEK/ICASE Joint Conference*., pp. 105~ 109.

Hirai, K., Hirose, M., Haikawa, Y. and Takenaka, T., 1998, "The Development of Honda Humanoid Robot," *IEEE Int. Conf. on Robotics and Automation,* Leuven, Belgium, pp. 1321~1326.

Lim, S., Kim, K. I., Son, Y. I. and Kang, H. I., 2005, "Walk Simulations of a Biped Robot," *ICCAS 2005*, Koyang, Korea, pp. 2132~2137.

Lim, S. and Ko, I., 2005, "Development and Application of a ZMP Sensor System," *Spring Conf. of KSME,* Busan, Korea, pp. 1376~1381.

Loffler, K., Gienger, M. and Pfeiffer, F., 2003, "Sensor and Control Design of a Dynamically Stable Biped Robot," *IEEE Int. Conf. on Robotics and Automation,* Taipei, Taiwan, pp. 484, 490.

Mechanical Dynamics Inc., 2001, Basic ADAMS Full Simulation Training Guide.

Vukobratovic, M., Borovac, B., Surla, D. and Stokic, D., 1990, *Scientific Fundamentals of Robotics 7: Biped Locomotion,* Springer-Verlag.